

1 **Genome evolution and early introductions of the SARS-CoV-2 Omicron Variant**
2 **in Mexico**

3

4 Hugo G. Castelán-Sánchez¹, León P. Martínez-Castilla¹, Gustavo Sganzerla-
5 Martínez^{2,3}, Jesús Torres-Flores¹, Gamaliel López-Leal^{1†}

6

7 ¹ Programa de Investigadoras e Investigadores por México. Grupo de Genómica y Dinámica Evolutiva
8 de Microorganismos Emergentes. Consejo Nacional de Ciencia y Tecnología. Av. Insurgentes Sur
9 1582, Crédito Constructor, Benito Juárez, CP 03940, Ciudad de México, México.

10 ² Laboratory of Immunity, Shantou University Medical College, Shantou, People's Republic of China

11 ³ The Department of Microbiology and Immunology Dalhousie University, Halifax, NS, Canada

12

13

14 Hugo G Castelán-Sánchez hugo.castelan@conacyt.mx

15 León P. Martinez-Castilla leon.martinez@conacyt.mx

16 Gustavo Sganzerla Martínez gustavo.sganzerla@dal.ca

17 Jesús Torres-Flores jesus.torres@conacyt.mx

18 Gamaliel Lopez-Leal gamaliel.lopez@conacyt.mx

19

20

21 † These authors contributed equally to this work

22 * Correspondence to: Hugo G. Castelán Sánchez hugo.castelan@conacyt.mx

23

24 **Keywords**

25 Omicron, introductions, natural selection, human mobility

26

27

28 **NOTE: This preprint reports new research that has not been certified by peer review and should not be used to guide clinical practice.**

29 **ABSTRACT**

30

31 A new variant of SARS-CoV-2 Omicron (Pango lineage designation B.1.1.529), was
32 first reported to the World Health Organization (WHO) by South African health
33 authorities on November 24, 2021. The Omicron variant possesses numerous
34 mutations associated with increased transmissibility and immune escape properties.
35 In November 2021, Mexican authorities reported Omicron's presence in the country.
36 In this study, we infer the first introductory events of Omicron and the impact that
37 human mobility can have on the spread of the virus. We also evaluated the adaptive
38 evolutionary processes in Mexican SARS-CoV-2 genomes during the first month of
39 circulation of Omicron.

40 We infer 173 introduction events of Omicron in Mexico in the first two months of
41 detection; subsequently, of the introductions, there was an increase in the prevalence
42 for January.

43 This higher prevalence of the novel variant results in a peak of cases reported, on
44 average, six weeks after a higher mobility trend was reported. The peak of cases
45 reported is due to the BA.1.1 Omicron sub-lineage dominated, followed by BA.1 and
46 BA.15 sub-lineages in the country from January to February 2022.

47 Additionally, we identified the presence of diversifying natural selection in the genomes
48 of Omicron and found mainly five non-synonymous mutations in the RDB domain of
49 the Spike protein, all of them related to evasion of the immune response. In contrast,
50 the other proteins in the genome are highly conserved—however, there are
51 homoplasies mutations in non-structural proteins, indicating a parallel evolution.

52

53

54

55 **1. INTRODUCTION**

56 The new coronavirus SARS-CoV-2, the causative agent of coronavirus disease 2019
57 (COVID-19), emerged at the end of 2019 in the province of Wuhan, China, and rapidly
58 spread to other countries, causing more than 5.2 million deaths worldwide as of
59 November 18, 2022 (Platto, Xue, y Carafoli 2020; Zhu et al. 2020). As new variants of
60 SARS-CoV-2 emerged in different regions of the world, the World Health Organization
61 (WHO) designated new variants as variants of interest (VOI), variants under
62 monitoring (VUM), and variants of concern (VOC), depending on their epidemiological
63 and clinical behavior (Aleem, Akbar Samad, y Slenker 2022). The emergence of VOCs
64 has been of particular interest because they are associated with remarkable increases
65 in the incidence of COVID-19 worldwide (Choi y Smith 2021). For example, the Alpha
66 (B.1.1.7), Gamma (P.1.X), and Delta (B.1.617.2) variants were associated with drastic
67 increases in the number of infections and COVID-19-related deaths in the United
68 Kingdom, Brazil, and India, respectively (Tao et al. 2021).

69 On November 24, 2021, health authorities in Botswana and South Africa reported
70 circulating a new SARS-CoV-2 variant that was later designated Omicron and
71 classified as a VOC by the WHO (Viana et al. 2022). This new variant displayed
72 several mutations across the genome, some previously found in other VOCs (Thakur
73 y Ratho 2022). One of the most critical traits of Omicron is the presence of a high
74 number of mutations (32 mutations) in the spike protein compared to other VOCs,
75 which might confer this variant an increased affinity towards the angiotensin-
76 converting enzyme 2(ACE2 receptor), enhancing entry into the host cell, and the ability
77 to escape neutralization by antibodies induced by either natural infection or

78 vaccination (Thakur y Ratho 2022). Moreover, recent *in vitro* studies reported that the
79 replication rates for Omicron are almost 70 times higher in bronchial tissue than in lung
80 tissue in contrast to the Delta variant, which might explain the high transmissibility of
81 Omicron (Chi-wai MC, Nicholls J, Pui-yan KH, Peiris M, Wah-Ching T, Lit-man LP s/f)
82 Omicron has already spread across 77 countries, and their genomes are available in
83 GISAID (Thakur y Ratho 2022). The Omicron variant was first detected in Mexico in
84 November 2021 and has rapidly spread since, probably causing the recent increase
85 in symptomatic COVID-19 cases observed in the country. Due to the high infectivity of
86 Omicron in contrast to other VOCs, the study of the evolution and transmission
87 patterns of this variant in different countries is crucial for the implementation of
88 effective strategies to reduce its impact in a clinical context. In this work, we focus on
89 identifying the first events of Omicron introduction to understand how the virus spreads
90 and spreads in Mexico, with which it is possible to identify more than 100 multiple
91 independent introductions. In addition, we analyzed adaptation signals throughout the
92 genome and found only evidence of natural selection in protein Spike and homoplasic
93 mutations in nonstructural proteins.

94

95 **2. MATERIALS AND METHODS**

96 **2.1 Collection of genomes**

97 Two hundred fifty-four complete Omicron genomes reported in Mexico were
98 downloaded between November 28 to December 27, 2021, from the Global Initiative
99 on Sharing All Influenza Data GISAID platform (<https://www.gisaid.org/>). Additionally,
100 the first 20 genomes of Omicron reported per country were downloaded. However,
101 there were fewer genomes available for some because there is no comprehensive

102 sequencing coverage. Finally, 2,148 Omicron SARS-COV-2 genomes sequenced
103 worldwide were analyzed (including 187 of other lineages to guide the phylogeny).
104 Additionally, to analyze the spread and diversification of Omicron in Mexico, genomes
105 of this GISAID variant were downloaded from November 2021 to April 2022 with the
106 parameters of inclusion, complete genome, high coverage, and low coverage
107 exclusion.

108

109 **2.2 Phylogenomics and phylogeographic analysis**

110 Genomes were aligned using MAFFT v7 software (Katoh, Rozewicki, y Yamada 2019),
111 trimming the 5' and 3' ends, and classified according to their viral lineage assignment
112 under the Pango nomenclature system using Pangolin v3.1.7, version (Rambaut et al.
113 2020).

114 To estimate the phylogenetic relationships and phylogeography between SARS-COV-
115 2 genomes, a maximum likelihood (ML) phylogenetic tree was constructed using the
116 IQ-Tree (Nguyen et al. 2015) under the GTR + G model of nucleotide substitution with
117 empirical base frequencies and four free site rate categories and statistical support (-
118 alrt 1000). Sequences from lineages other than Omicron were added to this phylogeny
119 to establish the monophyly of Omicron subtrees, while the sequences from Wuhan
120 were used to root the tree. The tree was evaluated for a temporal signal using
121 TempEst (Rambaut et al. 2016) (the outliers were eliminated).

122 A time-scaled phylogenetic tree was built with TreeTime v0.7.4 (Sagulenko, Puller, y
123 Neher 2018), which specified a clock rate of 8×10^{-4} substitutions per site per year
124 (s/s/y) according to the Nextstrain workflow (Hadfield et al. 2018).

125 The phylogeographic analysis detected and quantified Omicron lineage introduction
126 events into Mexico. This analysis was reconstructed from the time-scaled tree

127 generated previously with TreeTime v0.7.4. We use two different approaches based
128 on several models and inference methods. To identify independent introduction events
129 of Omicron in Mexico, we used a discrete diffusion model implemented in the software
130 package BEAST v1.10.4 (Drummond et al. 2012). The Bayesian analysis through
131 Markov chain Monte Carlo (MCMC) was run on 106 generations and sampled every
132 1,000 generations using the BEAST v1.10.4 tool. The time-scaled phylogeny
133 previously built was a fixed empirical tree and considered two possible ancestral
134 locations: "Mexico" and "other location," according to the described pipeline Dellicour
135 et al., 2021 (Dellicour, Durkin, et al. 2021, 2).

136 The MCMC convergence and mixing properties were inspected using Tracer v1.72
137 (Rambaut, A., Suchard, M.A., Xie, D. and Drummond, A.J. 2014, 6), and the effective
138 sample size (ESS) values above 200 were achieved for all parameters. The
139 phylogenies were annotated with a 10% burn-in by Tree Annotator. Subsequently, the
140 "Seraphim" package (Dellicour et al. 2016) extracted the Spatio-temporal information
141 from the data and visualized the phylogeographic reconstructions.

142 Second, we use PASTML (Ishikawa et al. 2019) briefly reconstructs the ancestral
143 character states and their changes along with the trees, with maximum likelihood
144 marginal posterior probabilities approximation (MPPA) and Felsenstein 1981 (F81)
145 model options. For the parameters in PASTML, we used MPPA as a prediction method
146 (standard settings). We added the character predicted by the joint reconstruction, even
147 if it was not selected by the Brier score (option forced_joint).

148 On the other hand, the Omicron sequences from Mexico that were downloaded from
149 November to April were built in to reconstruct a maximum likelihood phylogeny using
150 iqtree v.2.1.1, with the GTR+F+R3 substitution model and statistical support (-alrt
151 1000) and the phylogenetic tree was visualized in iTOL v5 (Letunic y Bork 2021).

152

153 **2.3 Daily mobility and cases report**

154 The mobility data used in this study was obtained from the Google Mobility Reports
155 service (<https://www.google.com/covid19/mobility/>) for all Mexican states. The data is
156 found in the following categories: *i*) grocery and pharmacy; *ii*) retail and recreation; *iii*)
157 parks; *iv*) workplaces; *v*) residential; *vi*) transit stations. The service has been updated
158 daily since 26-02-2020. The last date of collection was 17-04-2022. The data were
159 treated in weekly variations. Finally, we added up all six instances of mobility to come
160 up with a single unitary value representing the mobility of a given week.

161 The country was divided into seven regions to analyze the mobility as follows:
162 Northeast (NE; Coahuila, Nuevo León, and Tamaulipas), Northwest (NW; Baja
163 California, Baja California Sur, Chihuahua, Durango, Sonora, and Sinaloa) Central
164 North (CN; Aguascalientes, Guanajuato, Querétaro, San Luis Potosí, and Zacatecas),
165 Central South (CS; Mexico City, Estado de México, Morelos, Hidalgo, Puebla, and
166 Tlaxcala), West (W; Colima, Jalisco, Michoacán, and Nayarit), Southeast (SE;
167 Guerrero, Oaxaca, Chiapas, Veracruz, and Tabasco) and South (S; Campeche,
168 Yucatán, and Quintana Roo).

169 Moreover, daily cases of the COVID-19 transmission in Mexico were retrieved from
170 the service <https://datos.covid-19.conacyt.mx/>. The regionalized (please see above)
171 daily cases were analyzed in a 7-day window in order to eliminate data granularity.
172 Next, the data was converted into cases/100k inhabitants. All data analysis was
173 conducted through in-house R scripts.

174

175

176

177 **2.4 Natural Selection Analysis**

178 Natural selection can manifest in directional, diversifying, purifying, and episodic
179 selection. We evaluated these types of natural selection in Omicron genomes from
180 Mexico. The Omicron SARS-COV-2 genome was annotated using RCoV19
181 (<https://ngdc.cncb.ac.cn/ncov/?lang=en>) (Gong et al. 2020). The directional selection
182 search was performed with FEL (fixed effects likelihood), SLAC (single likelihood
183 ancestor counting) (Delport et al. 2010), and Fast Unconstrained Bayesian
184 AppRoximation (FUBAR), assuming that the selection pressure is constant across the
185 phylogeny for each site (Murrell et al. 2013). Furthermore, the episodic diversifying
186 selection was evaluated with the mixed-effects model (MEME) (Murrell et al. 2012).

187 **Homoplasy test**

188 We evaluated the sequences of Omicron (from Mexico) that have arisen independently
189 several times (homoplasies). Homoplasies are likely candidates for adaptation due to
190 convergent evolution, recombination, or errors during sequence data processing.
191 Homoplasies were detected on phylogeny using HomoplasyFinder (Crispell, Balaz, y
192 Gordon 2019). We collected all the Omicron sequences from Mexico and two
193 sequences from Bostwana (NICD-N22418 and NICD-N22397) as reference genomes.
194 Additionally, we used Snippy (<https://github.com/tseemann/snippy>) to detect single-
195 nucleotide variations (SNVs) using the Omicron genome NICD-N22418 as reference
196 genomes.

197

198 **3. RESULTS**

199 **3.1. Phylogenetic evidence for multiple introductions Omicron and the human**
200 **mobility facilitates its spread**

201 On December 3, 2021, the first WGS-confirmed case of symptomatic COVID-19
202 caused by Omicron (B.1.1.519) was reported by the Instituto Nacional de Diagnóstico
203 y Referencia Epidemiológica (InDRE), corresponding to a patient from South Africa
204 that arrived at Mexico City on 16 November 2021. Since then and up to December 27,
205 2021, 254 genomes were sequenced in Mexico, corresponding to the states of Baja
206 California ($n=1$), Chiapas ($n=1$), Guerrero ($n=1$), Hidalgo ($n=1$), Mexico City ($n=159$),
207 Oaxaca ($n=1$), Puebla ($n=4$), Quintana Roo ($n=18$), Sinaloa ($n=2$), State of Mexico
208 ($n=35$), Tabasco ($n=12$), Tamaulipas ($n=5$), Veracruz ($n=1$) and Yucatán ($n=13$).
209 Interestingly, most of the Omicron sequences come from Mexico City and the State of
210 Mexico, probably due to most international flights arriving in Mexico through the
211 country's capital. However, other states with international airports as well as important
212 tourist destinations such as Baja California Sur, Quintana Roo, Yucatán, and Sinaloa
213 also reported Omicron sequences and increases in cases in the first days of December
214 (**Figure S1**).

215 To determine Omicron introductions to Mexico, we constructed a phylogenetic tree
216 using 244 Omicron genome sequences from Mexico and 1903 foreign sequences
217 deposited in GISAID. First, we inferred phylogeny for said sequences, to trace the
218 movement of Omicron in Mexico through time and space. First, we note that the
219 sequences of the Mexican genomes do not form a single clade but rather are scattered
220 throughout the tree, consistent with multiple introductions to the country; In Figure A,
221 the green branches correspond to the Mexican sequences, while the gray branches
222 correspond to international sequences.

223 Through a discrete phylogeographic analysis following the Dellicour pipeline,
224 introductions were evaluated (Dellicour, Durkin, et al. 2021). For this purpose, we used
225 a time-scaled phylogenetic tree, and subsequently, introduction events were identified

226 in the MCC tree with an associated HPD interval by reporting the number of
227 introduction events. The analysis detected a minimum number of 173 introduction
228 events of the Omicron lineage (95% HPD interval = [162.925-176.025]) identified from
229 the phylogenetic analysis of 244 samples collected in Mexico (**Figure 1A**).

230 The discrete phylogeographic analysis in BEAST show that the majority of
231 introductions were represented by singletons (80%) and formed three small
232 monophyletic clades composed of at least ten sequences from Mexico, corresponding
233 to the center of Mexico, where the virus possibly initially spread throughout the country,
234 driven by the mobility of people. However, the highest peak of Omicron in Mexico was
235 reached by mid-January 2022, which may have had a more significant number of
236 introductions.

237 The PastML analysis predicted Botswana as the location of the tree root of Omicron,
238 suggesting that the Omicron variant origin might have been in southern African.

239 Four main clusters emerged from the Botswana cluster; the oldest clusters were
240 located in Hong Kong, India, Australia, and South Africa (**Figure S2**), which could
241 indicate that the first transmissions and spreads of the virus were possibly in those
242 locations. After the Botswana cluster, there is the cluster of South Africa, which is
243 linked to one of India, from which a small cluster of Mexico emerges; this result
244 suggests that the first independent introductions of Omicron to Mexico (four
245 sequences) could have come from South Africa or India.

246 On the other hand, another small cluster from Mexico is connected to the Singapore
247 cluster, which comes from a large group from Hong Kong (**Figure S2**). These results
248 indicate that the introduction of the virus to Mexico could have been through different
249 locations in Africa, India, and Asia. This analysis showed that the sequences of these

250 regions share similarities with the first sequences of Mexico, and possibly, this was
251 the spread of Omicron in the world towards Mexico.

252 As mentioned above, the peak of omicron was reached in mid-January 2022. A
253 maximum-likelihood phylogenetic tree was built on understanding the distribution of
254 Omicron during the increase in cases in the context of the first circulating genomes in
255 Mexico. We found multiple introductions of different Omicron sublineages, which are
256 marked with a red star in the phylogeny (**Figure 1B**).

257 The first genomes that circulated during the months of November and December
258 belong to the Omicron sub-lineages, a total of 244 genomes. **BA.1** 23.3% (n=57),
259 **BA.1.1** 39% (n=97), **BA.1.1.10** 0.4% (n=1), **BA.1.13** 0.4% (n=1), **BA.1.15** 29.91%
260 (n=73), **BA.1.17** 1.6% (n=4), **BA.1.17.2** 0.4% (n=1), **BA.1.18** 0.81% (n=2), and **BA.1.7**
261 4.9% (n=12).

262 These lineages were identified for the first time in Mexico City. For example, **BA.1** on
263 16/11/2021 imported from South Africa; **BA.1.1** on 19/11/2021; **BA.1.1.10** on
264 21/12/2021. **BA.1.17** on 18/12/2021, **BA.1.17.2** on 16/12/2021, and **BA.1.18** on
265 10/12/2021. While **BA.1.15** was first identified on 03/12/2021 in Tamaulipas.
266 Therefore, most of the introductions of the lineages are from the center of the country,
267 and these introductions spread to the rest of Mexico.

268 In the tree, the first genomes are distributed within the clades of the omicron sub-
269 lineages, indicating that these first introductions gave rise to the spread of the variant
270 throughout the country. However, not all introductory lineages reached a high
271 frequency, such as **BA.1.7**, **BA.1.8**, **BA.1.17.2**. Otherwise, lineages **BA.1**, **BA.1.1**, and
272 **BA.1.15** were the introductions that dominated and increased their frequency during
273 the Omicron peak, which correspond to the largest clades in the phylogenetic tree
274 (**Figure 1B**).

275 Interestingly, lineage BA.1.1 is subdivided into two large clades (clades in color Blue),
276 followed by lineage BA.1.5 distributed in three clades (Green), followed by BA.1 (red),
277 the most ancestral lineage in the tree. In contrast, the other lineages are found in a
278 lesser proportion (**Figure 1B**).

279 We also investigated whether the introduction and spread of the Omicron variant could
280 be due, in part, to trends of increased population mobility (**Figure 2**). We obtained
281 human mobility data and divided the country into seven regions NE, NW, CN, CS, W,
282 SE, and S. First, we found a mobility peak in December 2021 (**Figure 2-A**), involving
283 all Mexican regions. The mobility increase observed in December 2021 is the highest
284 observed in the Omicron selection period. Second, in **Figure 2-B** shows the increase
285 in reported cases in January 2022. Next, in **Figure 2-C**, we analyze the correlation
286 between increased mobility resulting in future cases. On average, it took six weeks for
287 the correlation between the two variables to start showing a stronger correlation
288 (except in the Northwest region). To explain the odd behavior of the Northwest region,
289 in **Figure S3** the mobility of the states of Baja California, Chihuahua, Durango, and
290 Sonora can be seen to increase earlier. Therefore, the earliest of these trends caused
291 the correlation of this region to be different than the others. In **Figure 2-D**, The Omicron
292 lineage peaked in mid-January 2022, where the B.1.1 lineage predominated
293 throughout the country, followed by the BA.1.15 and BA.1 lineages. Therefore, the
294 increase in cases is mainly associated with the BA.1.1 lineage. In addition, different
295 sub-lineages of Omicron have been established, which have not increased in
296 frequency, and perhaps many have become extinct.

297 As mentioned above, the peak of mobility increased in December 2021 in all regions
298 of Mexico; therefore, we also evaluated the prevalence and spread of omicron sub-
299 lineages over time in the seven regions (**Figure 3**). Initially, in November, the

300 prevalence of the Delta variant throughout the country was 99%. However, in
301 December, there was an increase in mobility, and most of the cases this month in the
302 Central and South region seem to be related to lineages BA.1 (~10.80%), BA.1.1
303 (~74.3%), and BA.1.15 (~11.25%). Whereas some states are located on the US-
304 Mexico border (Baja California, Chihuahua, Coahuila). On December NE and NW had
305 a higher prevalence of Delta (70%) than the Central-South and South states that
306 presented a 60% prevalence of Omicron sublineages. Subsequently, in January in all
307 regions, Omicron was already dominant with the three sub-lineages BA.1, BA.1.1, and
308 BA.1.1.15. Additionally, there was already a diversity of Omicron sub-lineages such
309 as BA.2 (first time detected on 9/01/2022 in Jalisco), BA.1.1.10, BA.1.17, BA.1.17.2,
310 BA.1.18 and BA.1.15. By February, BA.1.1 was already dominant over the other sub-
311 lineages in all regions, while BA.2 in March began to increase in frequency, especially
312 in the Central South and South regions.

313

314 **3.2 Analysis of natural selection of Omicron**

315 We then searched for evidence of positive selection in Omicron genomes isolated from
316 Mexico with different algorithms focused on a codon-based phylogenetic framework
317 by calculating the ratio of non-synonymous (dN) to synonymous (dS) substitutions per
318 coding sequence site (dN/dS). The evaluation of selection throughout the genome
319 revealed that sites are highly conserved and show no evidence of episodic and
320 directional selection. There was no evidence of an excess of non-synonymous
321 mutations (dN/dS>1), representing potential purifying selection pressure, except for
322 the gene encoding Spike. For the gene that codes for Spike protein, positive
323 diversifying selection was detected on five codon sites, and non-synonymous changes
324 in only five (dN/dS>1) through the FUBAR method, which assumes that the selection

325 pressure for each site is constant along the entire phylogeny with a Bayesian algorithm
326 to infer rates (dN/dS) (Murrell et al. 2013). Thus, genes were subjected to a distinct
327 natural selection strength.

328 The sites under positive natural selection found in the Spike gene were; L371S,
329 R346K, N417K, E484A, S496G, and N1098D (**Figure 4**). The L371S mutation (on
330 Spike) is within the receptor-binding domain (RBD, residues numbered 319–541). The
331 other observed mutations, R346K, N417K, E484A, and S496G are also found in the
332 RBD. Mutation R346K described in the Mu variant can alter the interactions with
333 monoclonal antibodies (Fratev 2022). Mutation E484A has been shown to confer up
334 to 10-fold greater resistance to vaccinee sera (Wang et al. 2021, 1). The mutations
335 L371S and S496G by neutral polar amino acid probably produce no difference in the
336 receptor's binding affinity (Rath, Padhi, y Mandal 2022). Finally, the N1098D mutation
337 occurs in the spike protein's S2 subunit (amino acid residues 686–1273). These
338 changes produced in the Spike protein by charged polar amino acids could have
339 significant repercussions, favoring a better interaction with the receptor. Interestingly,
340 these mutations may be local adaptations of the virus to the Mexican population.

341

342 **3.3 Detection of Homoplasies**

343 Homoplasies can be produced by base-pair substitutions or by recombination and can
344 emerge naturally in the context of neutral evolution or positive natural selection. In
345 order to detect homoplasies in the Omicron sequences in Mexico, we used
346 HomoplasmyFinder [24]. We used 244 Omicron (Mexico) sequences to construct a
347 phylogeny, adding two South African genomes, NICD-N22418 and NICD-N22397, as
348 the reference genomes. We identified homoplasies at 25 different positions (**Figure**
349 **S4**), corresponding to 24.5% of the 102 polymorphic sites identified. Of these, 18 were

350 in the ORF1a nsp11 gene. In addition, the homoplasmy at position 15854 was in RNA
351 polymerase, and the rest of the homoplasies (at positions 1694 to 9870) were in the
352 non-structural proteins (nsp). The homoplasies detected tend to change for thymine
353 or cytosine (**Supplementary table S1**).

354 On the other hand, using SNIPPY (using NICD-N22418 and NICD-N22397 as
355 reference genomes), we found that the homoplasies at positions 1694, 2205, 5250,
356 5465 can be directly observed from the Botswana genomes, suggesting that the rest
357 of the homoplasies could be generated from the descendants of the internal nodes.

358

359 **4. DISCUSSION**

360 In this study, we performed a phylogenetic and phylogeographic analysis to infer
361 Omicron introductions in Mexico and how mobility might affect virus spread following
362 introductions. Subsequently, we analyzed the adaptive evolutionary processes in local
363 genomes during the first month of circulation of Omicron in Mexico. According to the
364 data obtained from the genomes collected, the earliest detected genomes come
365 mainly from Mexico City, the State of Mexico, Quintana Roo, and Yucatán, of which
366 the first of the reported cases was imported from South Africa. However, most of the
367 introduction cases in Mexico were singletons, which indicates multiple independent
368 introductions (173 independent introductions). These results are like those reported
369 during the first epidemic wave in New York City by Dellicour et al., 2021; discrete
370 phylogeographic analysis found 116 independent introductions in the city and
371 relatively small clades. These results show the heterogeneity of the virus to establish
372 local transmission successfully (Dellicour, Hong, et al. 2021). The multiple
373 introductions of variants to Mexico have already been explored in other lineages, such
374 as B.1.1.519 (Taboada et al. 2021) and Alpha (Zárate et al. 2022). For example, in the

375 Alpha lineage, the introductions probably came from the United States, contributing to
376 the spread of the Alpha lineage from the north to the south of the country (Zárate et
377 al. 2022)

378 However, in the case of Omicron, the increase in cases was in Mexico City, probably
379 due to the arrival of international flights. As inferred from the PastML phylogeographic
380 analysis, the Mexican clusters came from South Africa and India. The other
381 introductions came from Hong Kong or Singapore, and this lineage arose from South
382 Africa; Therefore, we argue that human mobility is a fundamental factor in introducing
383 variants to a country. South Africa *per se* is an important airport hub in the continent
384 (Newfarmer, Page, y Tarp 2018). An example of that is mobility data that shows that
385 there have been approximately 93 thousand trips from South Africa to other 30 non-
386 African regions by November 2021. Moreover, by the time the WHO had declared
387 Omicron as a VoC, the probability of importation of the new variant exceeded 50% in
388 North America, Europe, Middle East, and Oceania (Bai et al. 2021). Therefore,
389 people's inbound through international mobility is likely to be the introductory event of
390 new variants and viruses.

391 From the moment a novel variant arrives in a country, internal mobility is among the
392 factors that will facilitate its local transmission (Fakir y Bharati 2021; Oka, Wei, y Zhu
393 2021). We show that by observing a mobility increase and correlating it with the
394 number of cases. In the regions where the first introductions of Omicron likely
395 happened, i.e., Southwest, Northwest, and Central South, we observed that higher
396 mobility was associated with higher cases six weeks after. On top of that, we argue
397 that the mobility trends of a population follow a seasonal trend, as reported in
398 (Hoogeveen, Kroes, y Hoogeveen 2022), since our data depicts a movement peak in
399 the end-of-year season. Next, we show that the increase in cases reported in early

400 January 2022 was due to the variants BA.1.1, BA.1, and BA.15, and it seems that
401 there is no regionalization of the sub-lineages. And, the local transmission chains
402 could reflect the higher internal mobility observed in the Southwest and Central South
403 of the country; this has been observed in the Delta variant in Mexico [...].

404 Once knowing the introductions of omicron to Mexico, we evaluated the adaptive
405 changes in the genomes of Mexico. Since natural selection is one of the main
406 evolutionary forces that generate diversity and show signs of adaptation of an
407 organism, we evaluate the diversifying directional selection. We use FUBAR, which
408 shows better performance on SLAC and FEL (Delport et al. 2010; Murrell et al. 2013).
409 The results revealed six sites under positive selection on Spike protein ($dN/dS > 1$). The
410 residues under positive selection are located in RBD on spike protein surrounding the
411 receptor-binding site (R346K, L371S, K417N, E484A, S496G, and N1098D)
412 associated mainly with evasion of antibodies. For example, the R346K amino acid
413 change, previously detected in lineage Mu (B.1.621) (Laiton-Donato et al. 2021, 2) is
414 associated with increased resistance to convalescent plasma therapy, and less
415 neutralization of antibodies (Liu et al. 2022). The substitution R346K was previously
416 reported in genomes from Mexico City with a prevalence of 40% in the capital and
417 according to phylogenetic analyses, the sequences from Mexico City form a
418 monophyletic clade (Cedro-Tanda et al. 2022). Genomes with the R346K mutation
419 now designated as BA.1.1 sub-lineage (Mohandas et al. 2022) which predominated in
420 Mexico and spread throughout the country.

421 The amino acid substitution L371S has been associated with a significantly increased
422 binding affinity to human ACE2 (Kimura et al. 2022). The amino acid substitution
423 K417N has been previously reported in the Alpha and Gamma lineages, which
424 facilitates the escape of monoclonal antibodies (bamlanivimab/LY-CoV555) (Starr et

425 al. 2021, 016) and the escape of vaccine sera such as BNT162b2 (Hoffmann et al.
426 2021). The amino acid substitution E484A is under selection in genomes in Mexico;
427 this substitution was previously E484K in the Beta, Gamma, and Mu variants related
428 to the escape to neutralization of vaccines. Currently, mutation E484A is present in
429 Omicron, weakening the mAbs binding to escape the immune response (Shah y Woo
430 2022). The S496G amino acid change is related to evasion of mAbs binding (Kannan
431 et al. 2022).

432 In general, the sites under selection in the protein S of the Omicron variants in Mexico
433 are associated with the evasion of antibodies. In addition, several recent studies have
434 proven that natural selection is evident in the Spike a glycoprotein (Chaw et al. 2020;
435 Tang et al. 2020). Changes in the amino acid sequence of RBD can dramatically
436 impact the binding affinity of Spike for the ACE2 receptor, in addition to causing
437 infectivity and transmission of SARS-CoV-2.

438 The methods used to detect natural selection determined sites under selection in
439 Spike and not in other Omicron genome regions. However, ORF1ab, ORF3a, and
440 ORF8 proteins have been reported to have sites that evolve under positive natural
441 selection (Velazquez-Salinas et al. 2020). Many of the mutations can occur repeatedly
442 and independently throughout the genome several times (homoplasies), which
443 produce non-synonymous changes at the protein level, are candidates for possible
444 adaptation due to positive natural selection. Therefore, we evaluated the presence of
445 homoplasies, which are recurrent mutations in the genomes of Mexico; we found that
446 most of the changes were associated with the ORF1a nsp11 gene, RNA polymerase,
447 and non-structural proteins (nsp). The recurrent mutation signal in Orf1a, which
448 encodes the nonstructural proteins Nsp11 and Nsp13, has been previously reported

449 (van Dorp et al. 2020, 2). In our analysis, the Nsp11 was the recurrent gene with
450 homoplasies.

451

452 **5. CONCLUSIONS**

453 The analyses presented here show multiple introductions of omicron that took place
454 in different regions of central-southern Mexico, then spreading to the rest of the country
455 during the first months of its circulation. We have also gathered evidence to show that
456 higher levels of mobility may have facilitated the spread of the variant to the outer
457 regions of the country. Here, we show that the increased mobility at the end of the
458 year resulted in a peak of Omicron cases; on average, it started being observed six
459 weeks later. The identification of introductions is essential to determine the spread of
460 the virus in a country. It also highlights the presence of diversifying natural selection
461 in the Spike protein and the presence of homoplasies mutations in non-structural
462 proteins, which may be possible candidates for adaptation of the virus to the Mexican
463 population. It is crucial to identify possible adaptation signatures in SARS-CoV-2 for
464 the continued development of vaccines and treatments.

465

466 **Acknowledgments**

467 We thank to Consorcio Mexicano de Vigilancia Genómica (CoviGen).

468 We thank the submitting laboratories for generating the genetic sequence and
469 metadata and sharing it through the GISAID initiative, on which this research is based.

470 **Authors contributions**

471 HGCS conceived the initial study. HGCS, GLL, JTF and LMC designed the
472 experiments. HGCS, GLL, and GSM performed analysis. HGCS, GLL, GMS, JTF, and
473 LMC have contributed to the interpretation and discussion of the results. HCGS and

474 GLL wrote the first manuscript draft with editing from GMS, JTF, and LMC. The final
475 manuscript was approved by all authors.

476 Reference

- 477 Aleem, Abdul, Abdul Bari Akbar Samad, y Amy K. Slenker. 2022. "Emerging Variants of
478 SARS-CoV-2 And Novel Therapeutics Against Coronavirus (COVID-19)". En
479 *StatPearls*. Treasure Island (FL): StatPearls Publishing.
480 <http://www.ncbi.nlm.nih.gov/books/NBK570580/>.
- 481 Bai, Yuan, Zhanwei Du, Mingda Xu, Lin Wang, Peng Wu, Eric H. Y. Lau, Benjamin J. Cowling,
482 y Lauren Ancel Meyers. 2021. "International risk of SARS-CoV-2 Omicron variant
483 importations originating in South Africa". *medRxiv*, diciembre, 2021.12.07.21267410.
484 <https://doi.org/10.1101/2021.12.07.21267410>.
- 485 Cedro-Tanda, Alberto, Laura Gómez-Romero, Guillermo de Anda-Jauregui, Dora Garnica-
486 López, Yair Alfaro-Mora, Sonia Sánchez-Xochipa, Eulices F. García-García, et al.
487 2022. "Early Genomic, Epidemiological, and Clinical Description of the SARS-CoV-2
488 Omicron Variant in Mexico City". *Viruses* 14 (3): 545.
489 <https://doi.org/10.3390/v14030545>.
- 490 Chaw, Shu-Miaw, Jui-Hung Tai, Shi-Lun Chen, Chia-Hung Hsieh, Sui-Yuan Chang, Shiou-
491 Hwei Yeh, Wei-Shiung Yang, Pei-Jer Chen, y Hurng-Yi Wang. 2020. "The Origin and
492 Underlying Driving Forces of the SARS-CoV-2 Outbreak". *bioRxiv*.
493 <https://www.biorxiv.org/content/10.1101/2020.04.12.038554v1>.
- 494 Chi-wai MC, Nicholls J, Pui-yan KH, Peiris M, Wah-Ching T, Lit-man LP. s/f. "HKUMed Finds
495 Omicron SARS-CoV-2 Can Infect Faster and Better than Delta in Human Bronchus but
496 with Less Severe Infection in Lung". Consultado el 12 de abril de 2022.
497 <https://www.med.hku.hk/en/news/press/20211215-omicron-sars-cov-2-infection>.
- 498 Choi, Jun Yong, y Davey M. Smith. 2021. "SARS-CoV-2 Variants of Concern". *Yonsei Medical*
499 *Journal* 62 (11): 961–68. <https://doi.org/10.3349/ymj.2021.62.11.961>.
- 500 Crispell, Joseph, Daniel Balaz, y Stephen Vincent Gordon. 2019. "HomoplasyFinder: a simple
501 tool to identify homoplasies on a phylogeny". *Microbial Genomics* 5 (1): e000245.
502 <https://doi.org/10.1099/mgen.0.000245>.
- 503 Dellicour, Simon, Keith Durkin, Samuel L. Hong, Bert Vanmechelen, Joan Martí-Carreras,
504 Mandev S. Gill, Cécile Meex, et al. 2021. "A Phylodynamic Workflow to Rapidly Gain
505 Insights into the Dispersal History and Dynamics of SARS-CoV-2 Lineages". *Molecular*
506 *Biology and Evolution* 38 (4): 1608–13. <https://doi.org/10.1093/molbev/msaa284>.
- 507 Dellicour, Simon, Samuel L. Hong, Bram Vrancken, Antoine Chaillon, Mandev S. Gill, Matthew
508 T. Maurano, Sitharam Ramaswami, et al. 2021. "Dispersal Dynamics of SARS-CoV-2
509 Lineages during the First Epidemic Wave in New York City". *PLOS Pathogens* 17 (5):
510 e1009571. <https://doi.org/10.1371/journal.ppat.1009571>.
- 511 Dellicour, Simon, Rebecca Rose, Nuno R. Faria, Philippe Lemey, y Oliver G. Pybus. 2016.
512 "SERAPHIM: Studying Environmental Rasters and Phylogenetically Informed
513 Movements". *Bioinformatics* 32 (20): 3204–6.
514 <https://doi.org/10.1093/bioinformatics/btw384>.
- 515 Delport, Wayne, Art F. Y. Poon, Simon D. W. Frost, y Sergei L. Kosakovsky Pond. 2010.
516 "Datamonkey 2010: a suite of phylogenetic analysis tools for evolutionary biology".
517 *Bioinformatics* 26 (19): 2455–57. <https://doi.org/10.1093/bioinformatics/btq429>.
- 518 Dorp, Lucy van, Mislav Acman, Damien Richard, Liam P. Shaw, Charlotte E. Ford, Louise
519 Ormond, Christopher J. Owen, et al. 2020. "Emergence of Genomic Diversity and
520 Recurrent Mutations in SARS-CoV-2". *Infection, Genetics and Evolution* 83
521 (septiembre): 104351. <https://doi.org/10.1016/j.meegid.2020.104351>.
- 522 Drummond, Alexei J., Marc A. Suchard, Dong Xie, y Andrew Rambaut. 2012. "Bayesian
523 Phylogenetics with BEAUti and the BEAST 1.7". *Molecular Biology and Evolution* 29
524 (8): 1969–73. <https://doi.org/10.1093/molbev/mss075>.

- 525 Fakir, Adnan M. S., y Tushar Bharati. 2021. "Pandemic Catch-22: The Role of Mobility
526 Restrictions and Institutional Inequalities in Halting the Spread of COVID-19". *PLOS*
527 *ONE* 16 (6): e0253348. <https://doi.org/10.1371/journal.pone.0253348>.
- 528 Fratev, Filip. 2022. "R346K Mutation in the Mu Variant of SARS-CoV-2 Alters the Interactions
529 with Monoclonal Antibodies from Class 2: A Free Energy Perturbation Study". *Journal*
530 *of Chemical Information and Modeling* 62 (3): 627–31.
531 <https://doi.org/10.1021/acs.jcim.1c01243>.
- 532 Gong, Zheng, Jun-Wei Zhu, Cui-Ping Li, Shuai Jiang, Li-Na Ma, Bi-Xia Tang, Dong Zou, et al.
533 2020. "An Online Coronavirus Analysis Platform from the National Genomics Data
534 Center". *Zoological Research* 41 (6): 705–8. [https://doi.org/10.24272/j.issn.2095-](https://doi.org/10.24272/j.issn.2095-8137.2020.065)
535 [8137.2020.065](https://doi.org/10.24272/j.issn.2095-8137.2020.065).
- 536 Hadfield, James, Colin Megill, Sidney M. Bell, John Huddleston, Barney Potter, Charlton
537 Callender, Pavel Sagulenko, Trevor Bedford, y Richard A. Neher. 2018. "Nextstrain:
538 real-time tracking of pathogen evolution". *Bioinformatics* 34 (23): 4121–23.
539 <https://doi.org/10.1093/bioinformatics/bty407>.
- 540 Hoffmann, Markus, Prerna Arora, Rüdiger Groß, Alina Seidel, Bojan F. Hörnich, Alexander S.
541 Hahn, Nadine Krüger, et al. 2021. "SARS-CoV-2 Variants B.1.351 and P.1 Escape
542 from Neutralizing Antibodies". *Cell* 184 (9): 2384-2393.e12.
543 <https://doi.org/10.1016/j.cell.2021.03.036>.
- 544 Hoogeveen, Martijn J., Aloys C. M. Kroes, y Ellen K. Hoogeveen. 2022. "Environmental
545 Factors and Mobility Predict COVID-19 Seasonality in the Netherlands". *Environmental*
546 *Research* 211 (agosto): 113030. <https://doi.org/10.1016/j.envres.2022.113030>.
- 547 Ishikawa, Sohta A., Anna Zhukova, Wataru Iwasaki, y Olivier Gascuel. 2019. "A Fast
548 Likelihood Method to Reconstruct and Visualize Ancestral Scenarios". *Molecular*
549 *Biology and Evolution* 36 (9): 2069–85. <https://doi.org/10.1093/molbev/msz131>.
- 550 Kannan, Saathvik R., Austin N. Spratt, Kalicharan Sharma, Anders Sönnernborg, Subbu
551 Apparsundaram, Christian Lorson, Siddappa N. Byrareddy, y Kamal Singh. 2022.
552 "Complex Mutation Pattern of Omicron BA.2: Evading Antibodies without Losing
553 Receptor Interactions", abril. <https://doi.org/10.20944/preprints202204.0120.v1>.
- 554 Katoh, Kazutaka, John Rozewicki, y Kazunori D. Yamada. 2019. "MAFFT online service:
555 multiple sequence alignment, interactive sequence choice and visualization". *Briefings*
556 *in Bioinformatics* 20 (4): 1160–66. <https://doi.org/10.1093/bib/bbx108>.
- 557 Kimura, Izumi, Daichi Yamasoba, Hesham Nasser, Jiri Zahradnik, Yusuke Kosugi, Jiaqi Wu,
558 Kayoko Nagata, et al. 2022. "SARS-CoV-2 Spike S375F Mutation Characterizes the
559 Omicron BA.1 Variant". Preprint. Microbiology.
560 <http://biorxiv.org/lookup/doi/10.1101/2022.04.03.486864>.
- 561 Laiton-Donato, Katherine, Carlos Franco-Muñoz, Diego A. Álvarez-Díaz, Hector Alejandro
562 Ruiz-Moreno, José A. Usme-Ciro, Diego Andrés Prada, Jhonnatan Reales-González,
563 et al. 2021. "Characterization of the emerging B.1.621 variant of interest of SARS-CoV-
564 2". *Infection, Genetics and Evolution* 95 (noviembre): 105038.
565 <https://doi.org/10.1016/j.meegid.2021.105038>.
- 566 Letunic, Ivica, y Peer Bork. 2021. "Interactive Tree Of Life (iTOL) v5: an online tool for
567 phylogenetic tree display and annotation". *Nucleic Acids Research* 49 (W1): W293–
568 96. <https://doi.org/10.1093/nar/gkab301>.
- 569 Liu, Haolin, Pengcheng Wei, John W. Kappler, Philippa Marrack, y Gongyi Zhang. 2022.
570 "SARS-CoV-2 Variants of Concern and Variants of Interest Receptor Binding Domain
571 Mutations and Virus Infectivity". *Frontiers in Immunology* 13.
572 <https://www.frontiersin.org/article/10.3389/fimmu.2022.825256>.
- 573 Mohandas, Sreelekshmy, Pragya D. Yadav, Gajanan Sapkal, Anita M. Shete, Gururaj
574 Deshpande, Dimpal A. Nyayanit, Deepak Patil, et al. 2022. "Pathogenicity of SARS-
575 CoV-2 Omicron (R346K) Variant in Syrian Hamsters and Its Cross-Neutralization with
576 Different Variants of Concern". *EBioMedicine* 79 (mayo).
577 <https://doi.org/10.1016/j.ebiom.2022.103997>.
- 578 Murrell, Ben, Sasha Moola, Amandla Mabona, Thomas Weighill, Daniel Sheward, Sergei L.
579 Kosakovsky Pond, y Konrad Scheffler. 2013. "FUBAR: A Fast, Unconstrained

- 580 Bayesian Approximation for Inferring Selection”. *Molecular Biology and Evolution* 30
581 (5): 1196–1205. <https://doi.org/10.1093/molbev/mst030>.
- 582 Murrell, Ben, Joel O. Wertheim, Sasha Moola, Thomas Weighill, Konrad Scheffler, y Sergei L.
583 Kosakovsky Pond. 2012. “Detecting Individual Sites Subject to Episodic Diversifying
584 Selection”. *PLoS Genetics* 8 (7): e1002764.
585 <https://doi.org/10.1371/journal.pgen.1002764>.
- 586 Newfarmer, Richard, John Page, y Finn Tarp, eds. 2018. *Industries without Smokestacks:
587 Industrialization in Africa Reconsidered*. WIDER Studies in Development Economics.
588 Oxford: Oxford University Press.
589 [https://oxford.universitypressscholarship.com/10.1093/oso/9780198821885.001.0001](https://oxford.universitypressscholarship.com/10.1093/oso/9780198821885.001.0001/oso-9780198821885)
590 /oso-9780198821885.
- 591 Nguyen, Lam-Tung, Heiko A. Schmidt, Arndt von Haeseler, y Bui Quang Minh. 2015. “IQ-
592 TREE: A Fast and Effective Stochastic Algorithm for Estimating Maximum-Likelihood
593 Phylogenies”. *Molecular Biology and Evolution* 32 (1): 268–74.
594 <https://doi.org/10.1093/molbev/msu300>.
- 595 Oka, Tatsushi, Wei Wei, y Dan Zhu. 2021. “The Effect of Human Mobility Restrictions on the
596 COVID-19 Transmission Network in China”. *PLOS ONE* 16 (7): e0254403.
597 <https://doi.org/10.1371/journal.pone.0254403>.
- 598 Platto, Sara, Tongtong Xue, y Ernesto Carafoli. 2020. “COVID19: An Announced Pandemic”.
599 *Cell Death & Disease* 11 (9): 1–13. <https://doi.org/10.1038/s41419-020-02995-9>.
- 600 Rambaut, A., Suchard, M.A., Xie, D. and Drummond, A.J. 2014. “Tracer v1.6”.
- 601 Rambaut, Andrew, Edward C. Holmes, Áine O’Toole, Verity Hill, John T. McCrone,
602 Christopher Ruis, Louis du Plessis, y Oliver G. Pybus. 2020. “A Dynamic Nomenclature
603 Proposal for SARS-CoV-2 Lineages to Assist Genomic Epidemiology”. *Nature
604 Microbiology* 5 (11): 1403–7. <https://doi.org/10.1038/s41564-020-0770-5>.
- 605 Rambaut, Andrew, Tommy T. Lam, Luiz Max Carvalho, y Oliver G. Pybus. 2016. “Exploring
606 the Temporal Structure of Heterochronous Sequences Using TempEst (Formerly Path-
607 O-Gen)”. *Virus Evolution* 2 (1): vew007. <https://doi.org/10.1093/ve/vew007>.
- 608 Rath, Soumya Lipsa, Aditya K. Padhi, y Nabanita Mandal. 2022. “Scanning the RBD-ACE2
609 molecular interactions in Omicron variant”. *Biochemical and Biophysical Research
610 Communications* 592 (febrero): 18–23. <https://doi.org/10.1016/j.bbrc.2022.01.006>.
- 611 Sagulenko, Pavel, Vadim Puller, y Richard A. Neher. 2018. “TreeTime: Maximum-Likelihood
612 Phylodynamic Analysis”. *Virus Evolution* 4 (1): vex042.
613 <https://doi.org/10.1093/ve/vex042>.
- 614 Shah, Masaud, y Hyun Goo Woo. 2022. “Omicron: A Heavily Mutated SARS-CoV-2 Variant
615 Exhibits Stronger Binding to ACE2 and Potently Escapes Approved COVID-19
616 Therapeutic Antibodies”. *Frontiers in Immunology* 12.
617 <https://www.frontiersin.org/article/10.3389/fimmu.2021.830527>.
- 618 Starr, Tyler N., Allison J. Greaney, Adam S. Dingens, y Jesse D. Bloom. 2021. “Complete map
619 of SARS-CoV-2 RBD mutations that escape the monoclonal antibody LY-CoV555 and
620 its cocktail with LY-CoV016”. *Cell Reports Medicine* 2 (4): 100255.
621 <https://doi.org/10.1016/j.xcrm.2021.100255>.
- 622 Taboada, Blanca, Selene Zárata, Pavel Iša, Celia Boukadida, Joel Armando Vazquez-Perez,
623 José Esteban Muñoz-Medina, José Ernesto Ramírez-González, et al. 2021. “Genetic
624 Analysis of SARS-CoV-2 Variants in Mexico during the First Year of the COVID-19
625 Pandemic”. *Viruses* 13 (11): 2161. <https://doi.org/10.3390/v13112161>.
- 626 Tang, Xiaolu, Changcheng Wu, Xiang Li, Yuhe Song, Xinmin Yao, Xinkai Wu, Yuange Duan,
627 et al. 2020. “On the origin and continuing evolution of SARS-CoV-2”. *National Science
628 Review* 7 (6): 1012–23. <https://doi.org/10.1093/nsr/nwaa036>.
- 629 Tao, Kaiming, Philip L. Tzou, Janin Nouhin, Ravindra K. Gupta, Tulio de Oliveira, Sergei L.
630 Kosakovsky Pond, Daniela Fera, y Robert W. Shafer. 2021. “The Biological and
631 Clinical Significance of Emerging SARS-CoV-2 Variants”. *Nature Reviews. Genetics*
632 22 (12): 757–73. <https://doi.org/10.1038/s41576-021-00408-x>.

- 633 Thakur, Vikram, y Radha Kanta Ratho. 2022. "OMICRON (B.1.1.529): A New SARS-CoV-2
634 Variant of Concern Mounting Worldwide Fear". *Journal of Medical Virology* 94 (5):
635 1821–24. <https://doi.org/10.1002/jmv.27541>.
- 636 Velazquez-Salinas, Lauro, Selene Zarate, Samantha Eberl, Douglas P. Gladue, Isabel
637 Novella, y Manuel V. Borca. 2020. "Positive Selection of ORF1ab, ORF3a, and ORF8
638 Genes Drives the Early Evolutionary Trends of SARS-CoV-2 During the 2020 COVID-
639 19 Pandemic". *Frontiers in Microbiology* 11 (octubre): 550674.
640 <https://doi.org/10.3389/fmicb.2020.550674>.
- 641 Viana, Raquel, Sikhulile Moyo, Daniel G. Amoako, Houriiyah Tegally, Cathrine Scheepers,
642 Christian L. Althaus, Ugochukwu J. Anyaneji, et al. 2022. "Rapid epidemic expansion
643 of the SARS-CoV-2 Omicron variant in southern Africa". *Nature* 603 (7902): 679–86.
644 <https://doi.org/10.1038/s41586-022-04411-y>.
- 645 Wang, Pengfei, Manoj S. Nair, Lihong Liu, Sho Iketani, Yang Luo, Yicheng Guo, Maple Wang,
646 et al. 2021. "Antibody Resistance of SARS-CoV-2 Variants B.1.351 and B.1.1.7".
647 *Nature* 593 (7857): 130–35. <https://doi.org/10.1038/s41586-021-03398-2>.
- 648 Zárate, Selene, Blanca Taboada, José Esteban Muñoz-Medina, Pavel Iša, Alejandro
649 Sanchez-Flores, Celia Boukadida, Alfredo Herrera-Estrella, et al. 2022. "The Alpha
650 Variant (B.1.1.7) of SARS-CoV-2 Failed to Become Dominant in Mexico". *Microbiology
651 Spectrum* 10 (2): e0224021. <https://doi.org/10.1128/spectrum.02240-21>.
- 652 Zhu, Na, Dingyu Zhang, Wenling Wang, Xingwang Li, Bo Yang, Jingdong Song, Xiang Zhao,
653 et al. 2020. "A Novel Coronavirus from Patients with Pneumonia in China, 2019". *New
654 England Journal of Medicine* 382 (8): 727–33.
655 <https://doi.org/10.1056/NEJMoa2001017>.
- 656

657

658 **Figure legends**

659 **Figure 1 - Phylogeography and Phylogenomics analysis Omicron.** A) Time-scaled analysis of
660 Omicron showing the 173 introduction events to Mexico, shown at the nodes in red color, and branches
661 color in green represent genomes sampled from Mexico. In contrast, the branches in gray correspond
662 to samples from other places. B) Maximum likelihood phylogeny of Omicron Mexican lineages, tips are
663 colored by lineage.

664

665 **Figure 2 - Mobility.** A) Google mobility trends (retail, recreation, grocery, pharmacy, parks, public
666 transport, workplace, and residential) of each Mexican region are computed from 2021-09-18 to 2022-
667 03-12. Mobility levels above 0 indicate a trend above the baseline. The baseline was a period of
668 observation from before the pandemic (the baseline day is the median value from the 5 week period
669 Jan 3 – Feb 6, 2020. B) Daily COVID cases are computed in each Mexican region from 2021-09-18 to
670 2022-03-12. C) Pearson and Spearman correlations between COVID cases and mobility are computed.
671 In order to analyze how long it takes for a spike in mobility to result in more cases, the cases were
672 assessed in n weeks in the future (after the mobility spike). D) Number of SARS-CoV-2 genomes

673 obtained at the national level. The BA.1.1 lineage was the most abundant in January and February.
674 BA.2 in March, it seems its frequency begins to increase.

675

676 **Figure 3 - Distribution of Omicron lineages in Mexico between November 2021 and April 2022.**

677 (A), Northeast (B), Central North (C), Central South (D), West (E), Southeast (F), and South (G). The
678 lineages B.1.1, B.1, and B.1.15 were predominant in all regions in January.

679

680 **Figure 4 - Spike protein model of Omicron SARS-COV.** The sites that will evolve under positive
681 selection according to FUBAR method are shown in red color.

682

683 **Figure Supplementary**

684

685 **Figure S1. Number of cases per 100,000 population.**

686 The number of cases per 1000 inhabitants in the first months of the introduction of omicron is shown in
687 each state of Mexico. The states of Baja California Sur, Mexico City, State of Mexico, Quintana Roo,
688 and Yucatan.

689

690 **Figure S2. Ancestral-state reconstruction using maximum likelihood inferred with PastML.**

691 Colors correspond to different countries. Numbers inside (or next to) the circles indicate the number of
692 strains assigned to the specific node, and the size of the circles is proportional to the number of tips.

693

694 **Figure S3. Mobility of Northwest region.**

695 The states composing the Northwest region were isolated in terms of their mobility trends in order to
696 explain the odd behavior of the mobility vs. cases correlation reported in the Northwest region by Figure
697 2-C. The mobility index reported is the result of the mobility categories Google displays (i.e., retail,
698 recreation, grocery, pharmacy, parks, public transport, workplace, and residential). The baseline
699 indicates how mobility used to be in the timespan of Jan 3 – Feb 6, 2020.

700

701

702

703 **Figure S4. Homoplasies in Omicron from Mexico.**

704 A phylogenetic tree was reconstructed using 244 Omicron genome sequences. The colored right
705 columns represent the 25 homoplasies identified. The nucleotides associated with these positions in
706 each sequence are plotted and colored according to their type (Adenine=red, Cytosine=blue,
707 Guanine=cyan, Thymine=orange, and no information for the nucleotide (Ns) = white). The tree's base
708 is in the NICD-N22418 and NICD-N22397 as reference genomes. Homoplasies are indicated in the
709 internal nodes (Mexican sequences).

710

711 **Supplementary Table S1**

712 Supplementary Table 1. The number of changes observed (multiple alleles present) for each of sites
713 on the phylogeny.

714

715

716

717

718

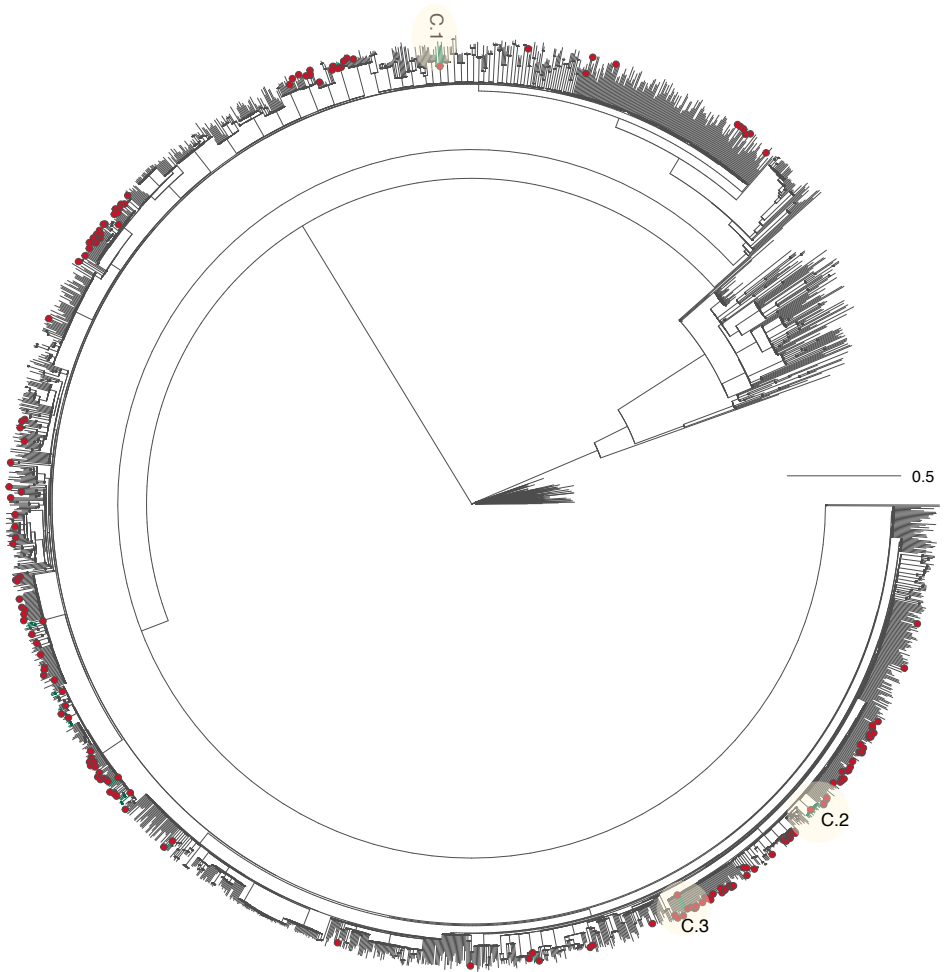
719

720

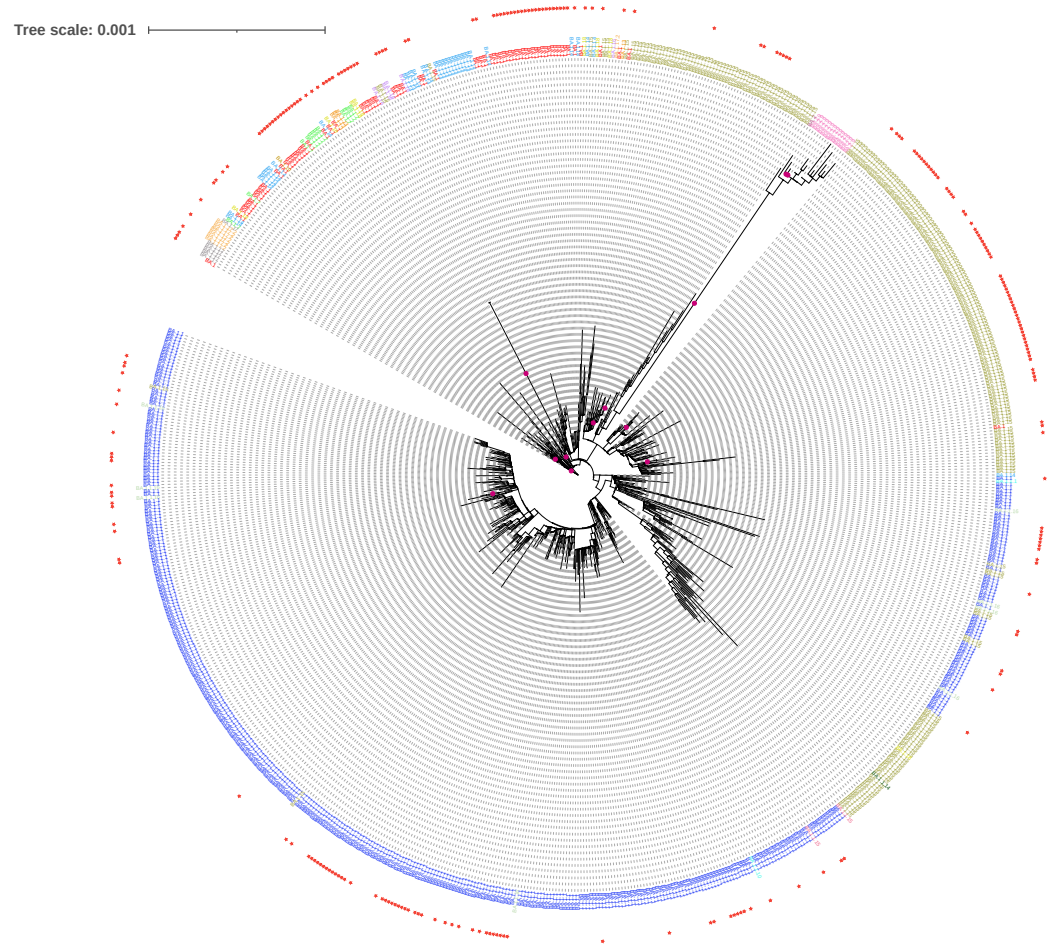
721

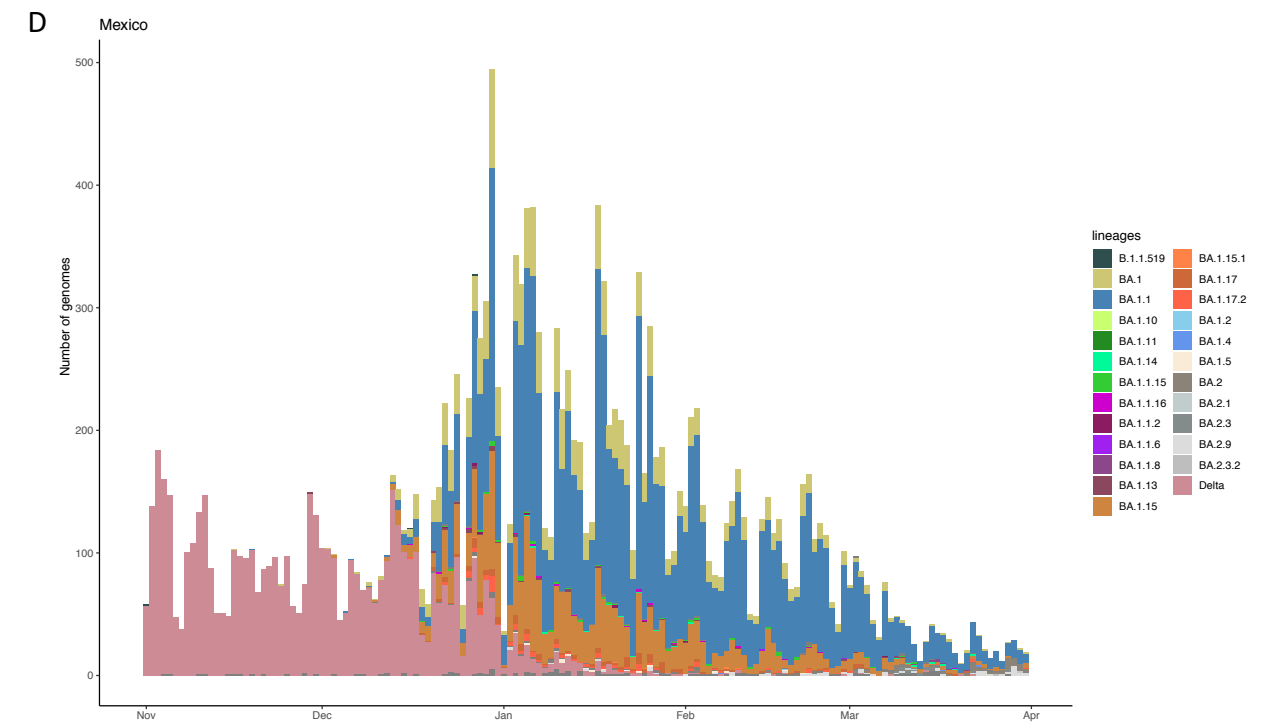
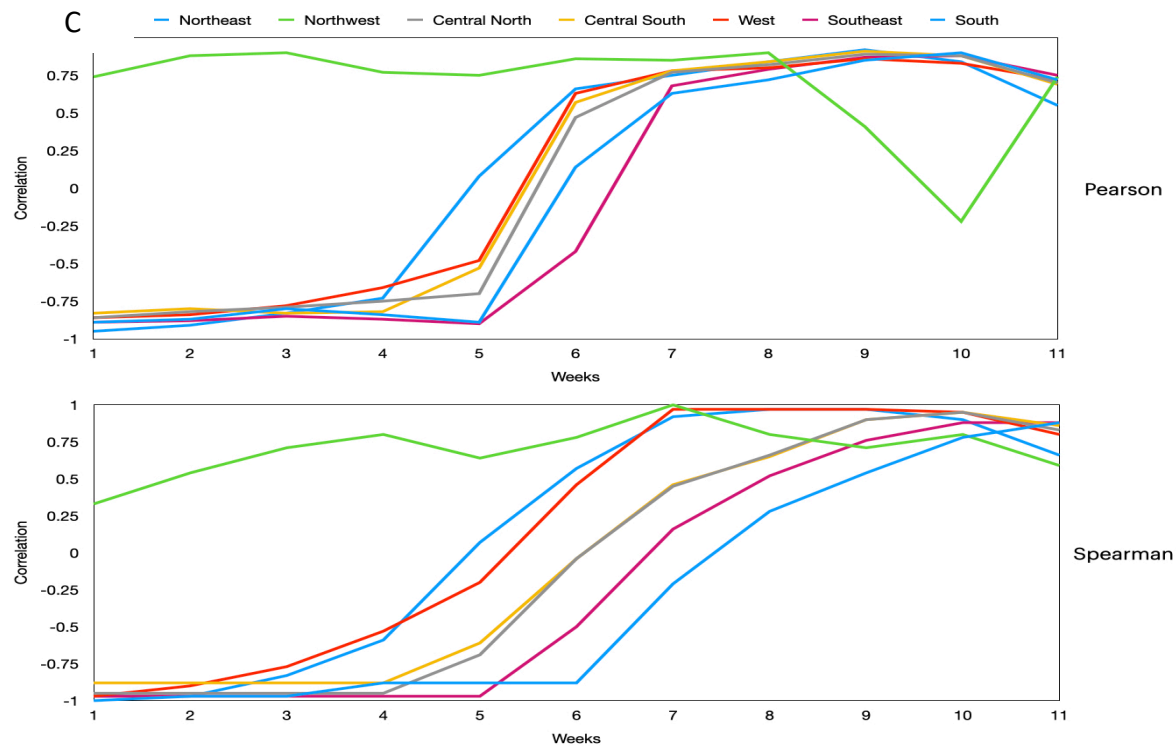
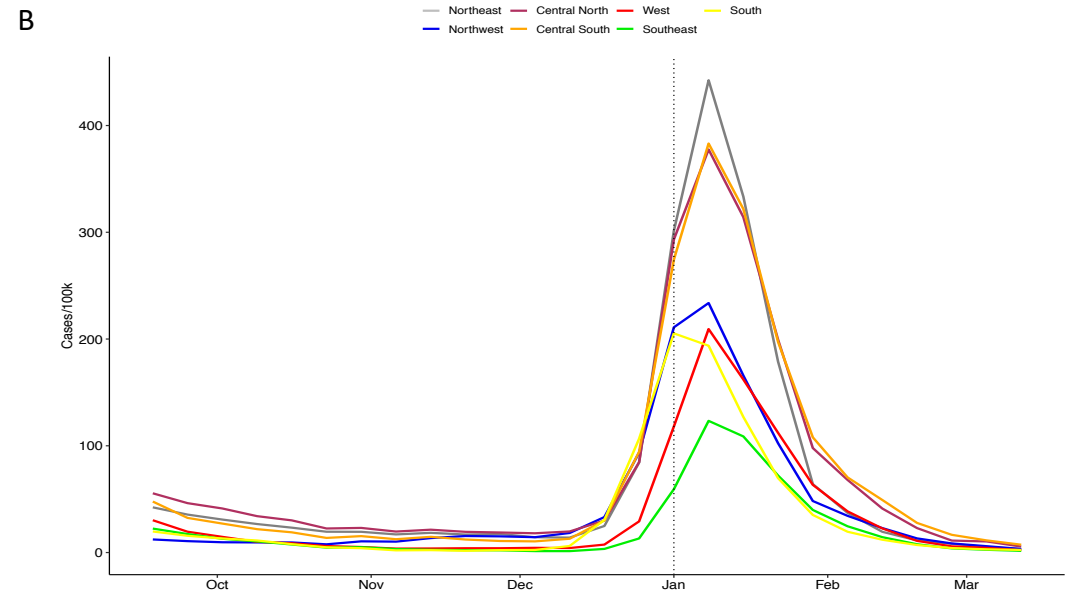
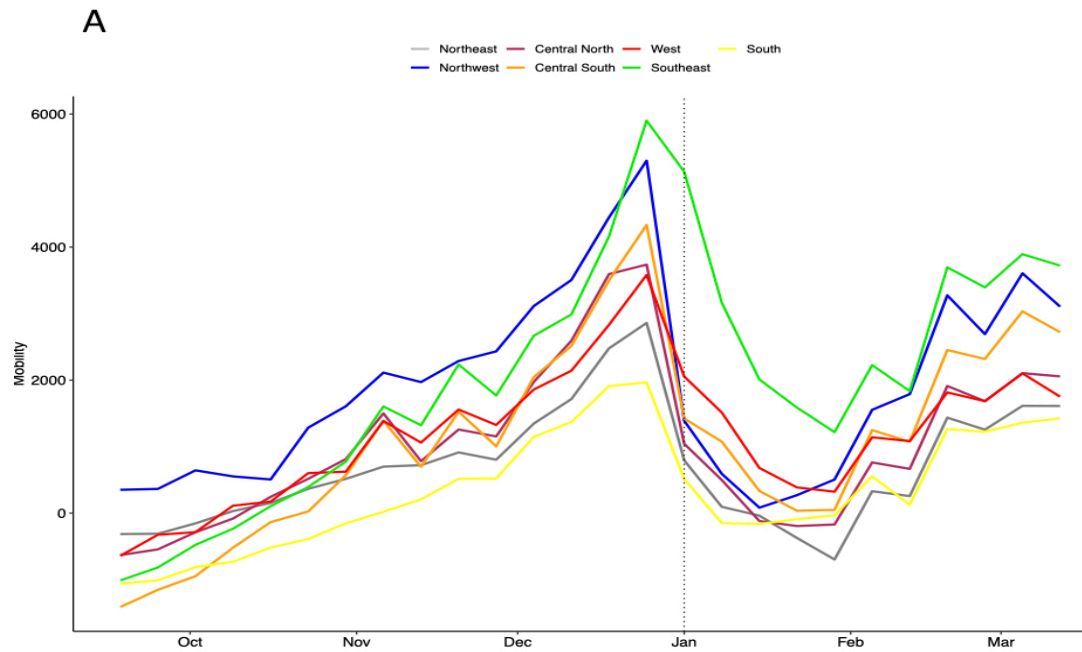
722

A

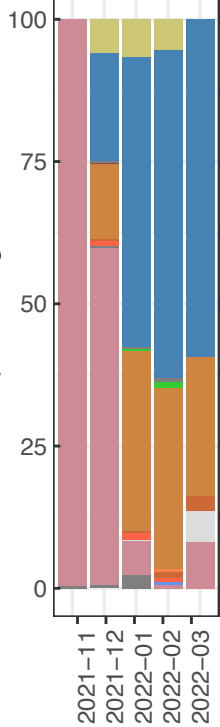


B

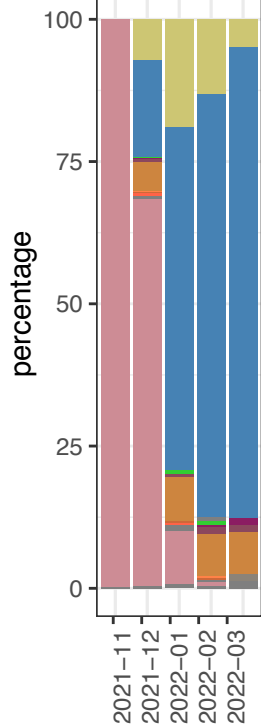




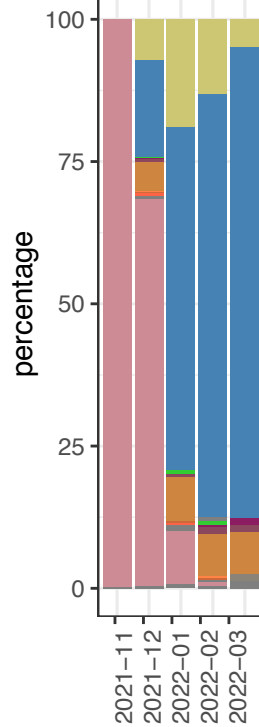
A. Northeast



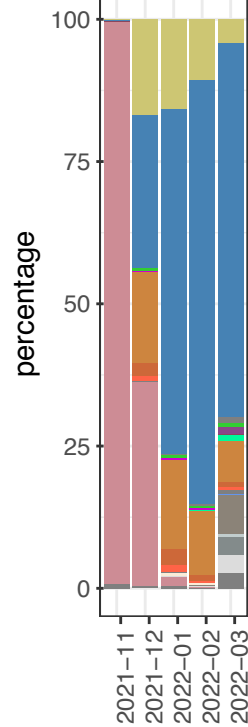
B. Northwest



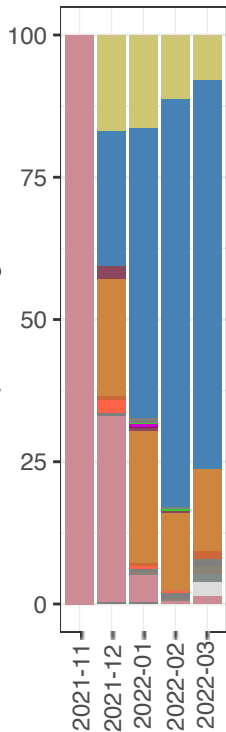
C. Central North



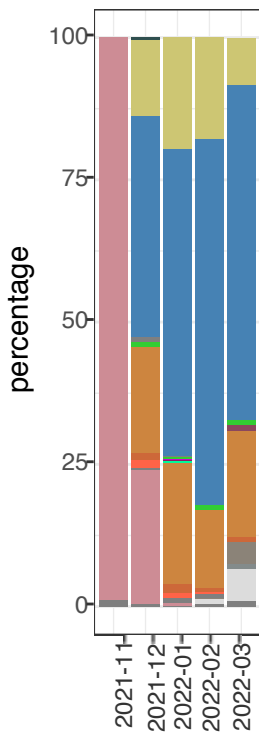
D. Central South



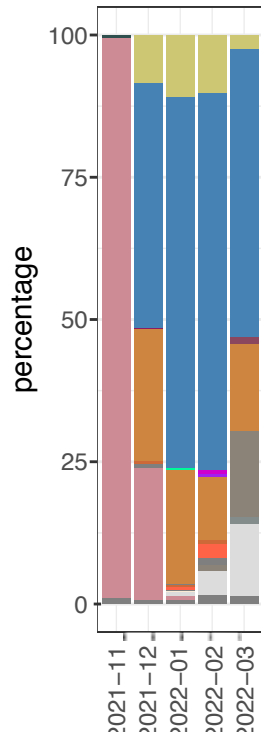
E. West



F. Southeast



G. South



Lineage

